Journal of Medicinal Chemistry

ARTICLE

pubs.acs.org/jmc

Structure−Activity Study To Develop Cationic Lipid-Conjugated Haloperidol Derivatives as a New Class of Anticancer Therapeutics

Krishnendu Pal,[†,∥] Subrata Kumar Pore,[†] Sutapa Sinha,[‡] Rajiv Janardhanan,[§] Debabrata Mukhopadhyay,[‡] and Rajkumar Banerjee*[,†]

[†]Division of Lipid Science and Technology, Indian Institute of Chemical Technology, Hyderabad, Andhra Pradesh 500007, India

[‡]Department of Biochemistry and Molecular Biology and [§]Department of Radiology, Mayo Clinic Foundation, Rochester, Minnesota 55902, United States

Supporting Information

ABSTRACT: Haloperidol (HP), a neuroleptic drug, shows high affinity toward σ receptors (SR). HP and reduced-HP at higher concentration were known to induce apoptosis in SR-overexpressing carcinomas and melanomas. Herein, we report the development of cationic lipid-conjugated haloperidol as a new class of anticancer therapeutics. In comparison to HP, the C-8 carbon chain analogue (HP-C8) showed significantly high, SR-assisted antiproliferative activity against cancer cells via caspase-3-mediated apoptosis and down-regulation of pAkt. Moreover, melanoma tumor aggressiveness in HP-C8-treated mice was significantly lower than that in HP-treated mice. HP-C8 simultaneously reduced Akt-protein level and increased Bax/Bcl-2 ratio in vascular endothelial cells, thereby indicating a possible protein kinase down-regulatory and apoptosis inducing role in tumor-associated vascular cells. In conclusion, we developed σ receptor-targeting cationic lipid-modified HP derivatives as a promising class of anticancer therapeutic that concurrently affects cancer and tumor environment associated angiogenic vascular cells through induction of apoptosis and Akt protein down-regulation.

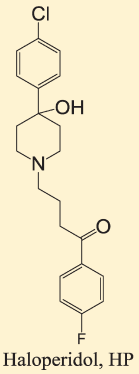

Haloperidol, HP

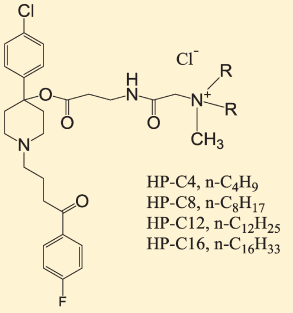

HP-C4, n-C_4H_9
HP-C8, n-C_8H_{17}
HP-C12, n-$C_{12}H_{25}$
HP-C16, n-$C_{16}H_{33}$

INTRODUCTION

σ receptors, a unique family of membrane-bound orphan receptor proteins, exist mainly in the central nervous system (CNS) but are expressed in various peripheral tissues at basal levels as well.[1,2] Moreover, tumor cell lines from diverse origins including neuroblastoma, glioma, melanoma, and carcinomas of breast, prostate, and lung overexpress σ receptors.[3−9] Interestingly, σ receptors are more highly expressed in rapidly proliferating cells and are down-regulated when cells become quiescent.[10,11] Their high density in various tumor cell types and particularly in rapidly proliferating cells makes σ receptors a potential target for diagnostic imaging and therapeutic agents.[8,9]

Several studies suggest that σ receptor agonists induce cell death in various tumor cell lines including prostate and breast carcinoma and melanoma, with features consistent with apoptosis.[12,13] Haloperidol (Scheme 1) is one of the σ receptor agonists that has been shown to inhibit cell proliferation and induce apoptosis in neuroblastomas, melanomas, and mammary and colon carcinomas in moderate concentrations.[12−15] Some recent studies attributed this cytotoxicity to haloperidol-induced Akt-sensitive mitochondrial translocation of proapoptotic Bcl-XS[14,15] and disruption of PI3K/PDK1/Akt pathway through differential subcellular compartmentalization of PI3K and PDK1.[16] However, in spite of the fact that haloperidol shows significant antiproliferative activity toward cancer cells, its full potential has never been realized through proper chemical modifications.

Recently we have shown that the targeting ability of haloperidol toward σ receptor remains potentially unchanged when the tertiary OH group of haloperidol is chemically conjugated to phospholipids with a PEG spacer between.[17] This observation prompted us to investigate whether the apoptosis inducing ability of haloperidol can be enhanced without hampering the targeting ability. To this end, we synthesized various haloperidol derivatives where the tertiary OH group of haloperidol was conjugated to cationic lipids of varying chain lengths. Twin carbon chain containing cationic lipids with its natural affinity toward predominantly negatively charged cell membrane bind and interact to transfer genes into cells and hence constitute a distinct class of gene delivery agents.[18] We hypothesized that upon conjugation of twin carbon chain cationic lipid to haloperidol, the resultant molecule will maintain its affinity for σ receptor and thus will not compromise its cellular entry in σ receptor overexpressing cancer cells. Moreover, the cellular entry may be further assisted by twin chain cationic lipids conjugated with it. This way the molecules' local concentration and availability inside the cell will be enhanced in comparison to unconjugated

Received: November 30, 2010
Published: March 10, 2011

Scheme 1. Structures of Haloperidol (HP), HP-C8, and C8 Control Molecule

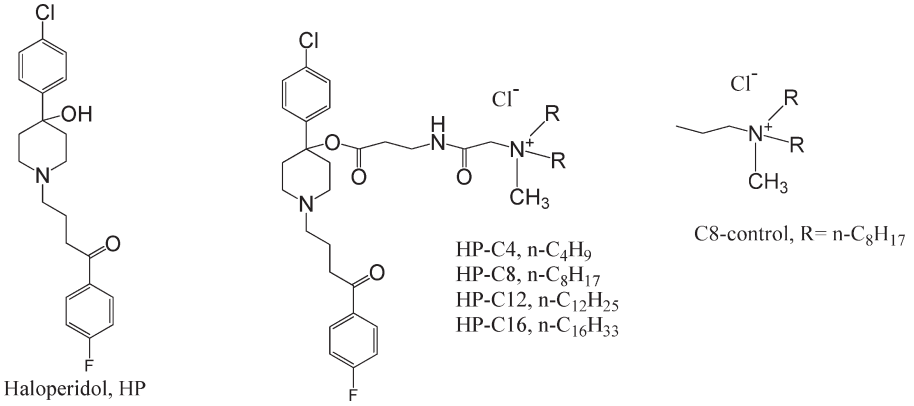

haloperidol and might help to induce rapid apoptosis at a given time of exposure.

Our investigation reported herein involves a detailed study of this new class of cationic haloperidol derivatives. At first, the most potent derivative was screened by testing against two σ receptor overexpressing breast cancer cell lines. Then the cytotoxicity of the selected derivative in four different cancer cell lines and two normal cell lines was evaluated and compared against that of unconjugated haloperidol. σ receptor mediated toxicity was confirmed by siRNA based down-regulation studies. FACS and further Western blot analyses showed induction of apoptosis via caspase 3 in cancer cells. Tumor model study and mechanistic study in vascular endothelial cells highlighted the molecules' multifunctional role in growth retardation of aggressive tumor.

RESULTS

Synthesis of Haloperidol Derivatives. Since the haloperidol derivatives differed only in chain lengths, a general procedure was used to synthesize them (Scheme 2a). At first the amine group of glycine *tert*-butyl ester was reacted with different haloalkanes in the presence of K_2CO_3 to obtain the respective tertiary amines (**1a**−**d**). This was followed by quaternization with methyl iodide to give the respective cationic lipid chains with iodide counterions (**2a**−**1d**). Then the ester protection of glycine moiety was removed using strong acid, TFA, to result in cationic lipids containing a free carboxylic acid group with trifluoroacetate counterion (**3a**−**d**). In a different reaction haloperidol was conjugated to *N*-Boc-β-alanine via DCC coupling to form haloperidol alanine ester (**4**). Then Boc-protection on the amine was removed to generate a free amine conjugated to haloperidol with a three-atom spacer (**5**). Finally, coupling of this amine with the carboxylic acid moiety of previously synthesized cationic lipids was achieved using HATU as a coupling reagent. This was followed by passing the resultant compound through chloride ion exchange resin, finally resulting in cationic haloperidol derivatives with different chain lengths (HP-C*n*, where n = 4, 8, 12, and 16).

For the synthesis of C8 control (Scheme 2b), at first dioctylamine (**7**) was synthesized by a nucleophilic reaction between octan-1-amine and 1-bromooctane. Then dioctylamine was reacted with 1-bromopropane to obtain a tertiary amine (**8**) which on quaternization with methyl iodide and successive chloride ion exchange with Amberlite IRA-400Cl resin yielded C8 control molecule **9**.

HP-C8 Exerts Maximum Toxicity toward Cancer Cells. We first chose two σ receptor expressing cancer cells, i.e., MCF-7 and MDA-MB-231, to screen the molecule with maximum toxicity to cancer cells. From the screening experiments it was clearly observed that among the four synthesized haloperidol derivatives HP-C8 has maximum toxicity toward human breast cancer cells, MCF-7 and MDA-MB-231 cells (Figure 1). In order of toxicity, HP-C12 is more toxic than HP-C16, but both of them are significantly less toxic than HP-C8 ($p < 0.001$) at therapeutic concentration range. The toxicity of HP-C4 is comparable to that of haloperidol. The experiment prompted us to select the eight-carbon chain derivative, HP-C8, for further characterization experiments.

HP-C8 Is More Toxic toward Cancer Cells Compared to Normal Cells. σ receptors are basally expressed in almost all kinds of cells. In this experiment we included a greater number of cancer cells compared to that in the screening experiment and also included two cells with noncancer lineage irrespective of their σ receptor expression status. This experiment was executed to show HP-C8's general efficacy as an anticancer molecule. HP-C8 shows significantly more toxicity ($p < 0.001$) toward all four cancer cells tested (MCF-7, MDA-MB-231, ZR-75-1, and B16F10) compared to either haloperidol or C8 control (Figure 2). IC_{50} values of HP-C8 for these cancer cells range from 2.5 to 3 μM. In normal cells (COS-1 and HEK-293), however, HP-C8 exhibited more or less similar toxicity compared to haloperidol or C8 control at concentrations less than 10 μM. IC_{50} values of HP-C8 for these normal cells vary from 7 to 7.5 μM (data not shown). Therefore, HP-C8 is 2−3 times more toxic toward cancer cells compared to normal cells. It is interesting to note that toxicities in cancer cells exhibited by individual treatment of haloperidol or C8-control molecule were significantly enhanced when HP-C8, the conjugate of HP and C8 control molecule, was administered. We also treated selected cancer cells with an equivalent mixture of HP and C8 control molecule (Figure S1 of Supporting Information). We found that the mixture had more toxicity than individual treatment of either of the components, i.e., HP or C8 control molecule. However, the toxicity due to the conjugate molecule, i.e., HP-C8, was significantly higher than that induced by the mixture of HP and C8. This clearly indicates that the efficient delivery of HP with the help of cell surface active cationic lipid certainly induces more HP-mediated toxicity but is not as efficient as the conjugated molecule.

Down-Regulation of σ Receptor Decreases Toxicity of HP-C8. For this study two cells, MCF-7 (σ receptor overexpressing

dx.doi.org/10.1021/jm101530j |*J. Med. Chem.* 2011, 54, 2378–2390

Scheme 2. Synthesis of Haloperidol Derivatives and C8 Control[a]

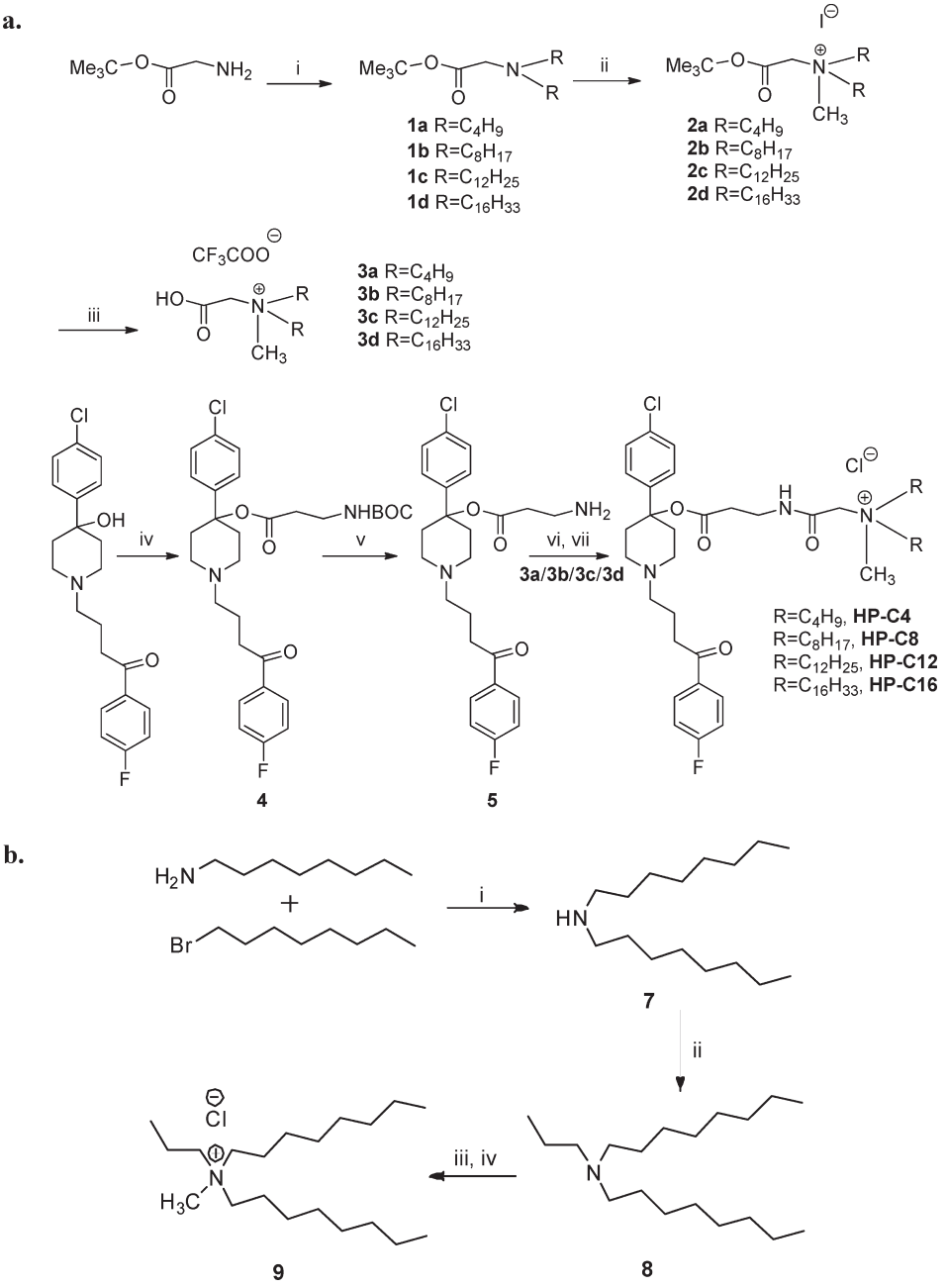

[a] Reagent and conditions for part a: (i) R-X, K_2CO_3, ethyl acetate, 70−80 °C; (ii) methyl iodide, dry DCM; (iii) 50% trifluoroacetic acid in dry DCM; (iv) *N*-Boc-*β*-alanine, dicyclohexylcarbodiimide (DCC), *N*,*N*-dimethylaminopyridine (DMAP), dry DCM; (v) 10% trifluoroacetic acid in dry DCM, 0 °C; (vi) [dimethylamino(triazolo[4,5-*b*]pyridine-3-yloxy)methylidene]dimethylazanium hexafluorophosphate (HATU), diisopropylethylamine (DIPEA), dry DMF; (vii) Amberlite IRA-400Cl resin, methanol. Reagents and conditions for part b: (i) K_2CO_3, DMSO, 70−80 °C; (ii) 1-bromopropane, K_2CO_3, ethyl acetate, 70−80 °C; (iii) methyl iodide, dry DCM; (iv) Amberlite IRA-400Cl resin, methanol.

cancer cell) and COS-1 (*σ* receptor basally expressing noncancer cell), were chosen. These cells were chosen to pinpoint any *σ* receptor-mediated anticancer effects of HP-C8. Hence, if HP-C8-mediated toxicity is *σ*-receptor-assisted, then the molecule should have the least toxicity in noncancer cells, which normally express the basal level of the *σ* receptor. They were treated with either siRNA against *σ* receptor subtype 1 or universal, control siRNA, following which the *σ* receptor levels in treated cells were respectively compared with the receptor levels of untreated cells (Figure 3a,b). Down-regulation of *σ* receptor in MCF-7 cells with *σ* receptor siRNA increases cell viability to a significant extent ($p < 0.001$) compared to untreated cells or control siRNA treated cells (Figure 3c). But the recovery in viability in HP-C8-treated *σ*-receptor-depleted cells was only moderate (25−30%) compared to *σ*-receptor-nondepleted cells. However, in antagonism based studies using ditolylguanidine (DTG), a nonspecific *σ* receptor antagonist, no such increase was observed (data not shown). This we presumed was due to greater affinity of HP-C8

dx.doi.org/10.1021/jm101530j |*J. Med. Chem.* 2011, 54, 2378–2390

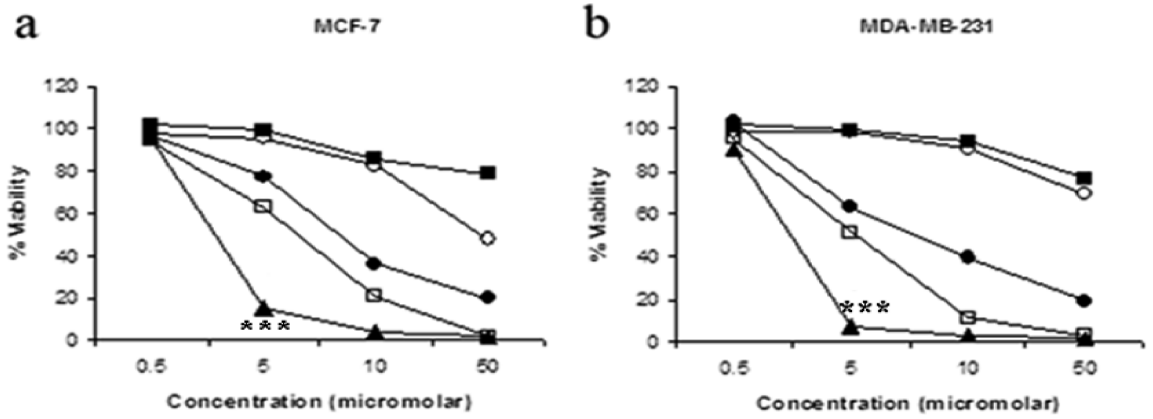

Figure 1. Viability studies of MCF-7 (a) and MDA-MB-231 (b) cells continuously treated with a range of concentrations of haloperidol (○), HP-C4 (■), HP-C8 (▲), HP-C12 (□), and HP-C16 (●), respectively, for 48 h. The asterisks (***) denote $p < 0.001$.

toward σ receptor compared to DTG, leading to irreversible binding of HP-C8 to σ receptors. On the other hand, by use of siRNA against σ receptor, the expression level of σ receptors decreases causing lesser amount of σ receptor-HP-C8 binding that ultimately leads to increase in cell viability. As expected, with no visible change in σ receptor level using siRNA in COS-1 cells there was no change in cellular viability, contrary to what is witnessed in cancer cells (Figure 3b,d). Here, σ receptor is expressed at a basal level and further down-regulation does not make a noticeable difference. In conclusion, the HP-C8-mediated toxicity in cancer cells is, at least partially, σ-receptor-dependent.

HP-C8 Induces Apoptosis in Cancer Cells but Not in Normal Cells. The apoptosis inducing effects of the HP-C8 were evaluated by annexin V/propidium iodide (PI) binding. One of the earliest events of apoptosis is the loss of plasma membrane integrity, accompanied by translocation of phosphatidylserine (PS) from the inner to outer membrane leaflets, thereby exposing PS to the external environment. The phospholipid binding protein annexin V has high affinity for PS and can bind to cells with externally exposed PS. Positive staining with fluorescently labeled annexin V correlates with loss of membrane polarity but precedes the complete loss of membrane integrity that accompanies the later stage of cell death resulting from either apoptosis or necrosis. In contrast, PI can only enter cells after loss of membrane integrity. Dual staining with annexin V and PI allows clear discrimination between unaffected cells (annexin V negative, PI negative, lower left quadrant), early apoptotic cells (annexin V positive, PI negative, lower right quadrant), late apoptotic cells (annexin V positive, PI positive, upper right quadrant), and necrotic cells (annexin V negative, PI positive, upper left quadrant). A higher amount of dual stained cells in the upper right quadrant indicates that the cells upon their initiation in apoptotic phase are in late apoptotic stage and there are significant losses of plasma membrane integrity that will result in their eventual death. In this experiment along with MCF-7 we chose to include B16F10 melanoma cells with which we made melanoma tumor model later. As can be seen in Figure 4, HP-C8 treatment (5 μM, 24 h) increases the percentage of late apoptotic cells (with both annexin V and PI positive staining, upper right quadrant) in MCF-7 and B16F10 cells whereas haloperidol (5 μM, 24 h) has no such effect. In normal cells like COS-1 and HEK-293 there are no differences between untreated cells and cells treated with haloperidol or HP-C8. Therefore, it is evident that HP-C8 treatment truly induced apoptosis specifically in cancer cells and did not induce apoptosis in normal cells.

Selective Tumor Regression by HP-C8 Compared to Haloperidol. To evaluate the tumor regression efficacy of HP-C8 compared to that of haloperidol in vivo, we made a subcutaneous model of B16F10 tumor in male C57BL6/J mice, divided them into two groups, and intraperitoneally injected either HP-C8 or haloperidol (at a dosage of 7.5 mg/kg) suspended in PBS containing 10% DMSO. The reason behind selection of this model is that B16F10 cells form rapidly growing tumors and had been shown to express high levels of σ receptor.[20] Figure 5a shows that a lesser amount of tumor growth is maintained in the HP-C8 treated group compared to the haloperidol treated group throughout the experiment. After five injections, the group treated with HP-C8 showed a significant regression in tumor growth ($P < 0.05$) compared to haloperidol treated group. Figure 5b shows the representative tumors from each group. After the completion of the experiment tumors from individual groups were cryosectioned and were imaged for relative density of apoptotic signs using TUNEL assay. Figure 5c shows that the tumor section obtained from HP-C8 treated group had more apoptotic regions compared to the tumor section obtained from the haloperidol treated group. Therefore, HP-C8 induced apoptosis not only in cancer cells in vitro but also in rapidly growing tumor tissues to result in significant inhibition of tumor growth.

HP-C8 triggers Intrinsic Pathway of Apoptosis and Phospho-Akt Down-Regulation in B16F10 Cells. The tumor model was made with B16F10, so we chose to see the mechanism of HP-C8 action in B16F10 cells. HP-C8 was treated with B16F10 in charcoal stripped serum condition to elucidate the mode of action of HP-C8 toward B16F10. In the intrinsic pathway of apoptosis the release of cytochrome *c* leads to activation of caspase 9 which finally cleaves procaspase 3 to release effector protein, activated caspase 3. The release of caspase 3 leads to apoptosis of cells. However, the release of cytochrome *c* is regulated by the Bcl-2 family of proteins. Members of this family such as Bax causes release of cytochrome *c*, thus acting as proapoptotic. But other antiapoptotic members of this family, such as Bcl-2, bind to pro-apoptotic Bax protein and inactivate them to release cytochrome *c*. So a higher value of Bax/Bcl-2 ratio indicates the onset of apoptosis in cells. As can be seen from Figure 6a, HP-C8 decreased the level of Bcl-2 expression and increased the expression of Bax in B16F10 cells in comparison to haloperidol (HP). The overall ratio of Bax/Bcl-2 obtained from

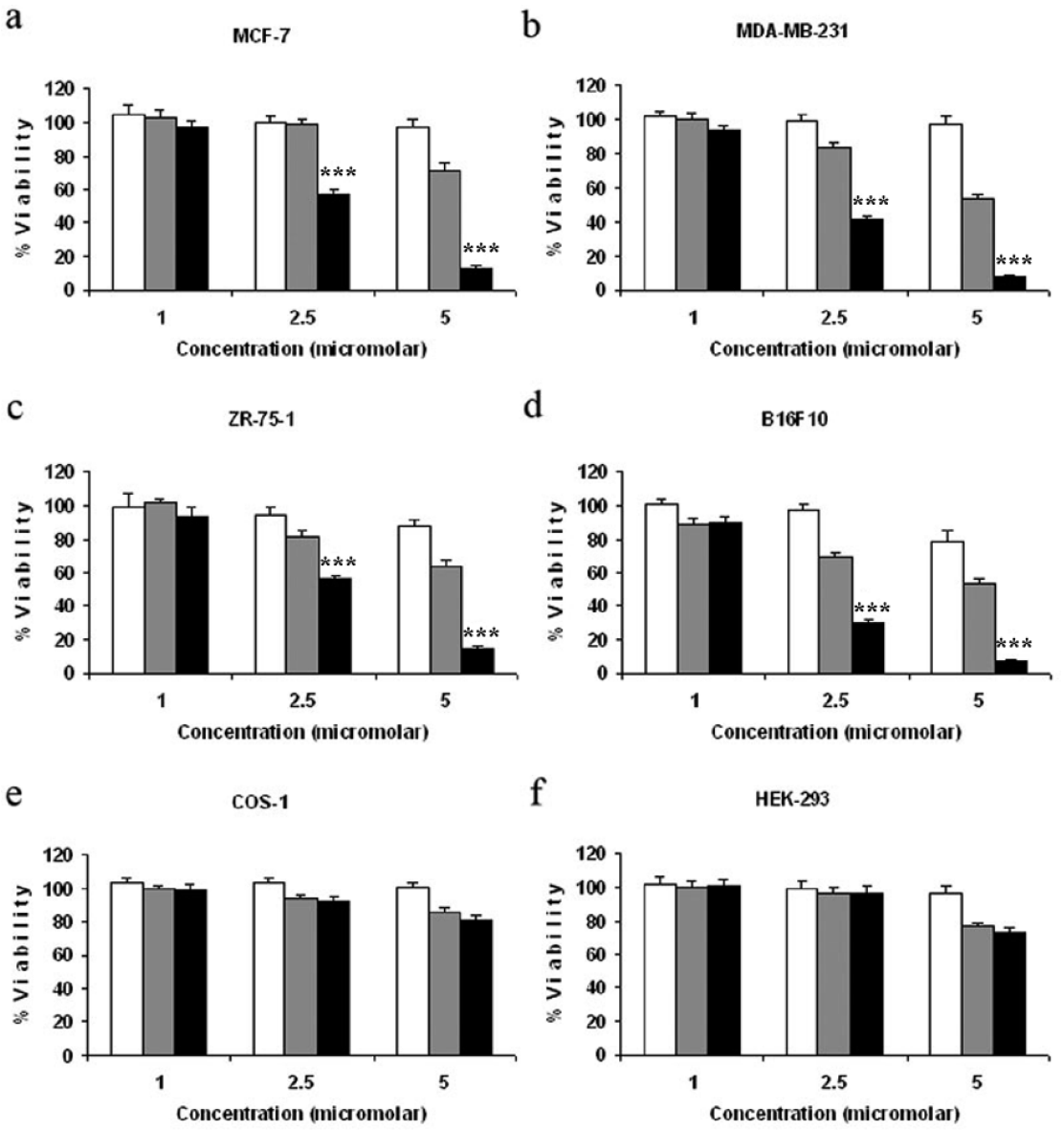

Figure 2. Viability studies of MCF-7 (a), MDA-MB-231 (b), ZR-75-1 (c), B16F10 (d), COS-1 (e), and HEK-293 (f) cells continuously treated with a range of concentrations of haloperidol (white bar), C8 control (gray bar), and HP-C8 (black bar), respectively, for 48 h. The asterisks (***) denote $p < 0.001$.

HP-C8-treated cells was almost doubled compared with that obtained from HP-treated cells. An elevated expression of cleaved (i.e., activated) caspase 3 was also observed in HP-C8 treated cells, indicating possible cytoplasmic release of cytotoxic cytochrome *c* from mitochondria or other proapoptotic factors. These eventually might have triggered intrinsic pathway of apoptosis which corroborates with a high level of toxicity to B16F10 cells as evidenced in viability studies (Figures 1 and 2) and flow cytometry data (Figure 4). Further, we found that HP-C8 could trigger the down-regulation of phospho-Akt production from Akt. Since a higher ratio of pAkt/Akt is linked with proproliferative pathways, this kinase down-regulatory property of HP-C8 might contribute to its anticancer action.

Mechanism of Action of HP-C8 in HUVEC Cells. Since excessive tumor growth is often accompanied by uninterrupted microangiogenesis and neovasculature formation, we suspected this phenomenon to assist the excessive growth and aggressiveness in B16F10 tumor. Since human umbilical vein endothelial cell (HUVEC) is a known model of angiogenesis/neovasculature, we chose to test the effect of HP-C8 on this cell. Figure 6b shows that HP-C8 clearly has detrimental effect on HUVEC cells. Clearly in contrast to HP, HP-C8 triggered the formation of cleaved caspase 3 followed by significant reduction of absolute amount of cellular Akt. As a result no phospho-Akt was formed in cells treated with HP-C8. The HP-C8-treatment apparently shut down the proproliferative Akt/pAkt pathway in the HUVEC cell. The up-regulation of caspase 3 in HP-C8-treated cell was further vindicated by the increase in Bax/Bcl-2 ratio. In conclusion, HP-C8 may have an inhibitory role in protein kinase B/Akt formation together with a role in triggering intrinsic pathway of apoptosis in vascular cells. This collective effect could have provided additional cause of tumor growth retardation owing to the killing of tumor-associated vascular cells.

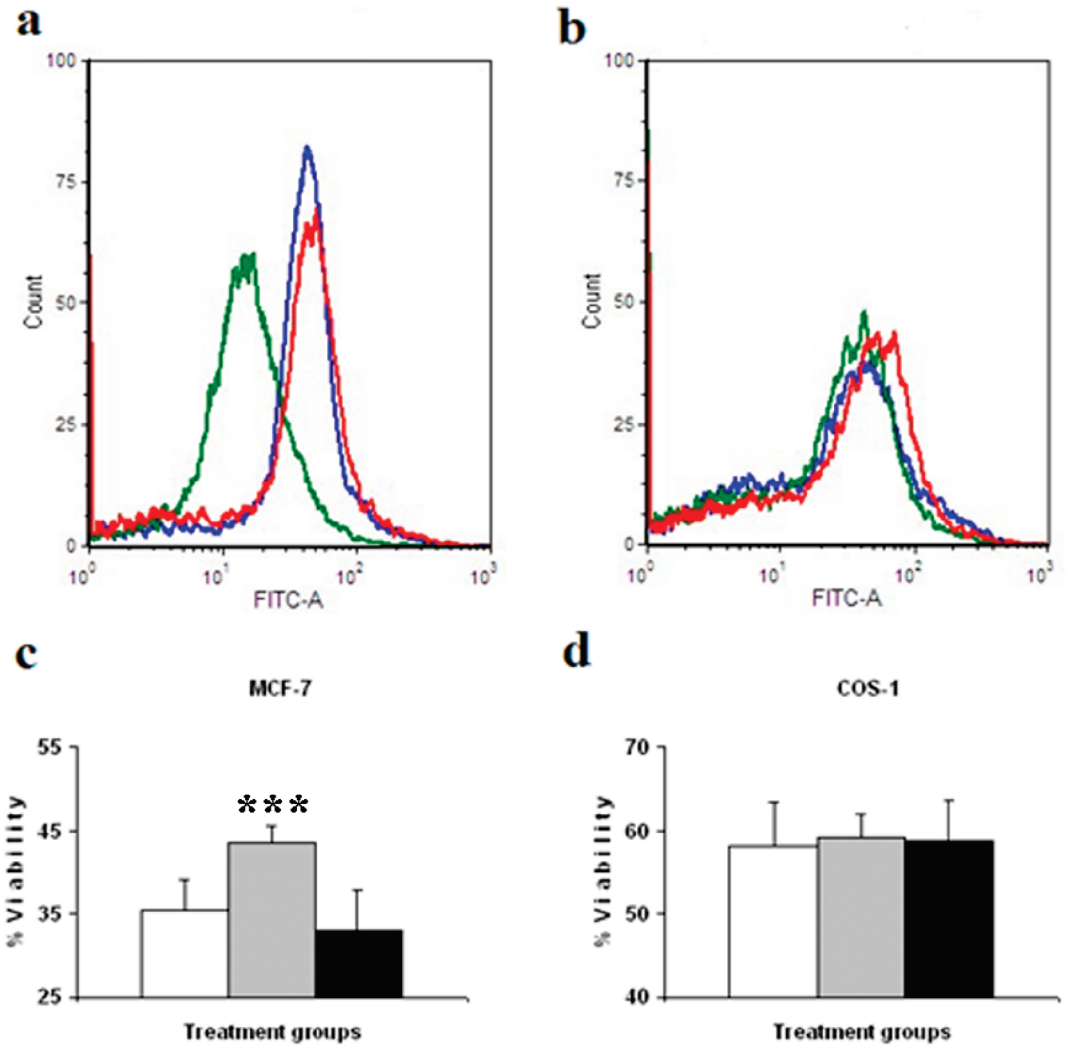

Figure 3. Flow cytometry analysis of σ receptor down-regulation in MCF-7 (a) and COS-1 (b) cells. Blue, green, and red lines represent untreated, σ receptor siRNA treated, and negative control siRNA treated cells, respectively. Parts c and d represent the viability data of MCF-7 and COS-1 cells obtained after 48 h following the treatment of 10 μM HP-C8 for 4 h. White, gray, and black bars represent SiRNA untreated, σ receptor siRNA treated, and negative control siRNA treated cells, respectively. The asterisk (*) denotes $p < 0.001$.

DISCUSSION

Development of newer class of drug candidates with multifunctional role for complicated diseases such as cancer is a challenging task. There are many existing drug molecules available with proven and time tested pharmacologic roles. These molecules are viable candidates for the development of newer drug molecules. Haloperidol is a well-known antipsychotic drug, but its usage following proper chemical modification for the treatment of cancer remained largely unutilized. Modification of haloperidol should be properly dealt with, since haloperidol is neurotoxic in nature through the possible down-regulation of antiapoptotic Bcl-2 or up-regulation of proapoptotic Bcl-XS.[21,22] Reduced haloperidol, which triggers cellular calcium release, was used for anticancer purposes, but this strategy was exploited limitedly.[23] We showed previously the first usage of neuropsychotic drug haloperidol (HP) for selectively targeting σ receptor overexpressing cancer cells if proper chemical modification could be accomplished.[17] Hypothesizing that better cellular interaction of haloperidol will increase its acceptability as an anticancer drug for σ receptor expressing cells, we chemically introduced the well-known cell-membrane-interacting cationic lipid component to accomplish this study.

We find that HP-C8, the eight-numbered-carbon-chain-linked haloperidol, has the maximum anticancer effect with minimal toxic effect to noncancer cells (Figures 1 and 2). A 2- to 3-fold difference in IC_{50} of HP-C8 in cancer cells with respect to currently selected normal cells is indeed concerning owing to narrow therapeutic window. Whether HP-C8 exhibits any specific antiproliferative effect against these chosen immortalized noncancer cells is a subject of further scrutiny in future. Further experiments with freshly isolated primary noncancer cells for determining actual therapeutic window are currently underway. However, this study clearly indicates predominant anticancer efficacy of HP-C8 which is substantiated in later experiments including in vivo experiments wherein apparently no HP-C8-induced toxicity is observed in mice during the course of treatment.

Further we find that this anticancer effect was at least partly mediated by σ receptor (Figure 3). The prominently higher percentage of postapoptotic cancer cells than normal cells treated

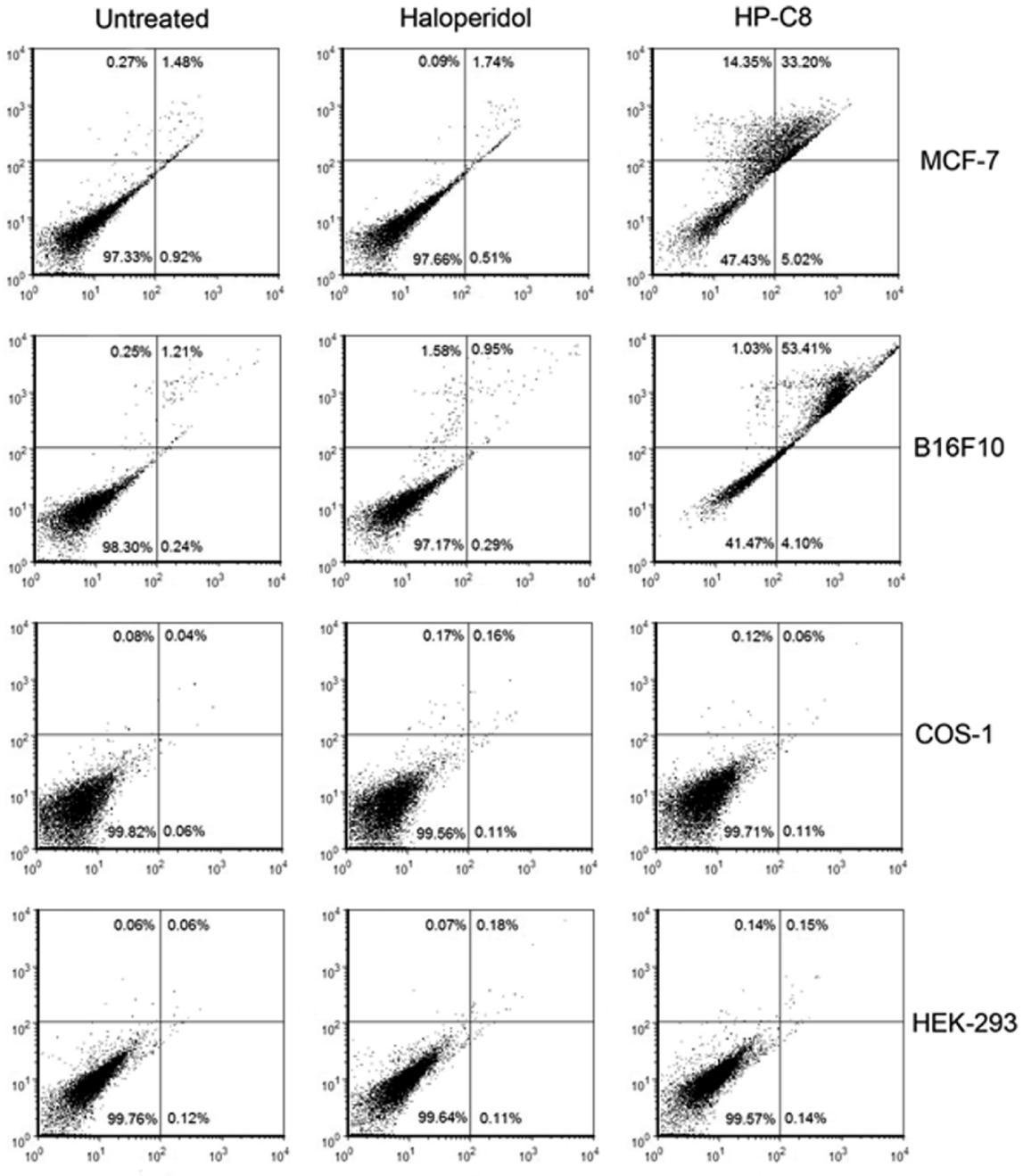

Figure 4. Flow cytometric analysis of apoptosis in MCF-7, B16F10, COS-1, and HEK-293 cells costained with FITC-annexin V/propidium iodide (PI). The horizontal and vertical axes represent FITC-annexin V and PI labeling, respectively. Cells were kept untreated or treated with 5 μM haloperidol or 5 μM HP-C8 for 24 h.

with HP-C8 (Figure 4) prompted us to investigate the pathway of apoptosis. The significant reduction in tumor aggression by HP-C8 in comparison to HP (Figure 5) indicated that beyond its toxic effect to cancer cells, the molecule might have detrimental effects on tumor-microenvironment-associated vascular endothelial cells. In all these experiments the parent molecule, HP, seems to have no specific anticancer role. This distinctive difference in anticancer property is certainly interesting and is expected to evoke strategies in future to modify pharmacologic drugs of similar pattern.

Further Western blot based studies revealed that in B16F10 melanoma cells HP-C8 triggered the intrinsic pathway of apoptosis, which is known to be initiated through the release of signal factors by mitochondria within the cell. Mitochondria integrate and propagate intracellular death signals originating from many factors including those induced by chemotherapeutic drugs.[24] This leads cytoplasmic, proapoptotic Bax, Bak, etc. proteins to bind to outer membrane of mitochondria and signal release of cytochrome *c*, which activates initiator protein caspase 9. Activated caspase 9 cleaves procaspase 3 to produce activated caspase 3, the effector protein that initiates cellular degradation. In contrast, Bcl-2, the antiapoptotic protein, down-regulates the release of cytochrome *c*.[25] Hence, a higher Bax/Bcl-2 ratio indicates the onset of apoptosis in cells. We found that the Bax/Bcl-2 ratio was nearly

dx.doi.org/10.1021/jm101530j |*J. Med. Chem.* 2011, 54, 2378–2390

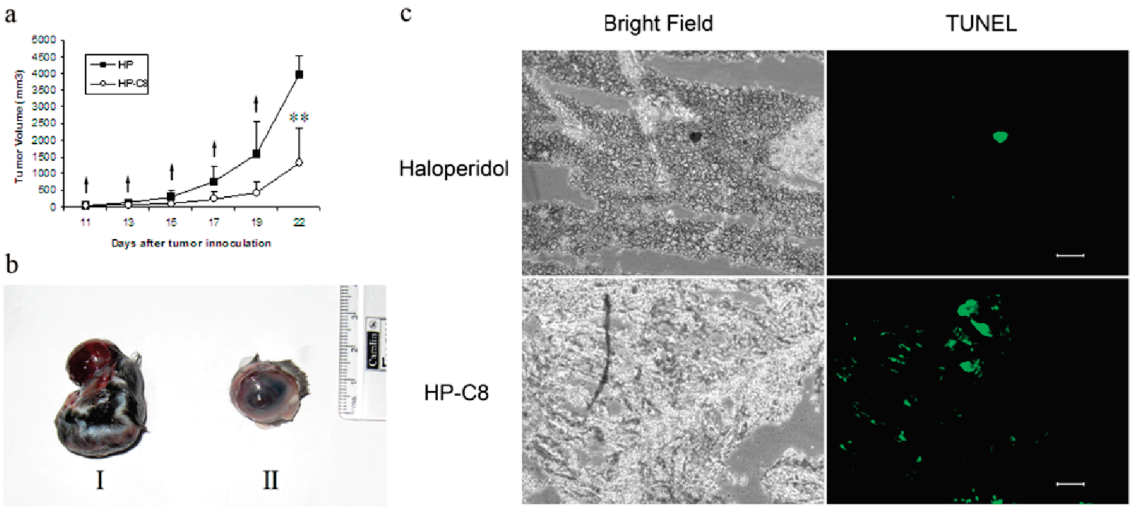

Figure 5. (a) Tumor growth curve after subcutaneous implantation of B16F10 cells in C57BL6/J mice followed by intraperitoneal injection of haloperidol (■) or HP-C8 (○) at a dosage of 7.5 mg/kg. The days of injections are indicated by black arrows. *Y*-axis denotes the size of tumors as tumor volume in mm^3, and *X*-axis denotes the number of days passed after tumor inoculation. ** denotes $p < 0.05$. (b) Representative samples of B16F10 tumors excised on day 23: (I) tumor from haloperidol treated group and (II) tumor from HP-C8 treated group. (c) Microscopic pictures of 10 μm tumor sections from haloperidol treated group (upper panel) and HP-C8 treated group (lower panel). Left panels show the tissue architecture in bright field, and right panels show the apoptotic regions in TUNEL assay. All the images are taken at 10× magnification. Bar = 2 μm.

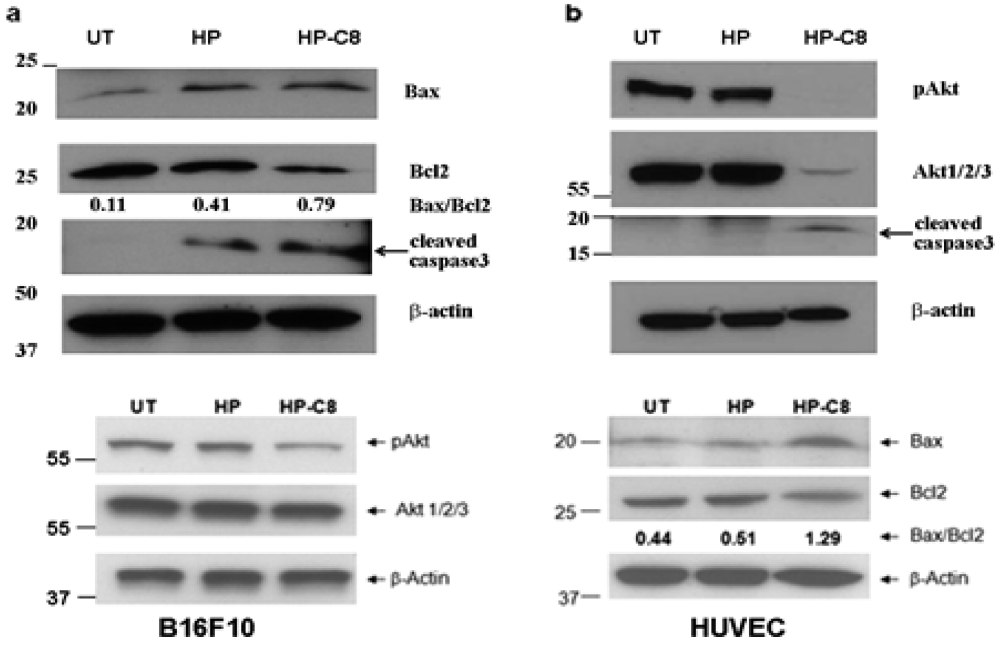

Figure 6. Western blot analysis. Differential expression of different regulators of apoptosis and proliferation in B16F10 (a) and HUVEC (b) cells treated with haloperidol (HP) and HP-C8 or kept untreated (UT).

doubled, resulting in concomitant release of more amount of activated caspase 3 in HP-C8-treated B16F10 cells than in HP-treated cells (Figure 6a). HP showed an increase in Bax/Bcl-2 ratio compared to untreated control, but it seems that this subtle increase could not evoke any visible anticancer effect. HP-C8 also induced apotosis in HUVEC cells, the viable model of cancer angiogenesis, through prominent up-regulation of Bax/Bcl-2 ratio with concomitant increase in caspase 3 (Figure 6b).

Another important regulator of apoptosis is Akt (protein kinase B, PKB), a family of serine/threonine kinases. Other activating kinases phosphorylate and activate this kinase. This prosurviving factor, i.e., activated Akt (pAkt), exerts many antiapoptotic activities, such as preventing release of cytochrome *c* from mitochondria, inactivating proapoptotic Fas ligand-expressing forkhead transcription factors, phosphorylating and inactivating proapoptotic factors BAD and pro-caspase-9, etc. Additionally, pAkt also mediates the activation of endothelial nitric oxide synthase (eNOS), an important modulator of angiogenesis.[26] In addition to the induction of apoptosis, HP-C8 played a kinase inhibitory role through down-regulation of the formation of pAkt in B16F10 cancer cells (Figure 6a). In HUVEC (Figure 6b), HP-C8 treatment inhibited the expression of Akt protein and hence probably the formation

dx.doi.org/10.1021/jm101530j |*J. Med. Chem.* 2011, 54, 2378–2390

of pAkt. Since Akt and pAkt are responsible for the activation of endothelial nitric oxide synthase (eNOS), an important modulator of angiogenesis, their absence leads to impaired angiogenesis. It remains to be seen if the inhibitory effect on eNOS activation indeed assists HP-C8 mediated growth inhibition of highly aggressive B16F10 melanoma tumors. Increase in activated caspase 3 in HP-C8-treated HUVEC could be partially vindicated by the increase in Bax/Bcl-2 ratio. However, the increase in caspase 3 with the complete inhibition of Akt formation may have a different implication. It is shown recently that the VEGF induction, which gives protection to Akt protein from proteasomal degradation, if inhibited, leads to down-regulation of Akt expression in HUVEC.[27] VEGF tyrosine kinase inhibitor or mTOR inhibitor rapamycin, even in the presence of VEGF stimulation, leads to a decrease in Akt protein expression in HUVEC cells, which is followed by the production of cleaved caspase 3.[27] In exact agreement with this published observation, HP-C8 induces a decrease in Akt expression and also increased production of cleaved caspase 3. This observation stands with a marked difference from what is observed when the mother molecule HP is treated to cells. However, it remains of further research interest to find if HP-C8 possesses a similar VEGF tyrosine kinase or mTOR inhibitory role. The data indicate the onset of apoptosis among the tumor vasculature which ultimately leads to inhibition of aggressiveness in tumor growth. Together, our data indicate that HP-C8 induces apoptosis not only in cancer cells but possibly also in adjoining vascular endothelial cells.

In conclusion, the findings of the present investigation demonstrate that structural modification of haloperidol by conjugation with a cationic lipid moiety indeed increases its apoptosis-inducing property in cancer cells without significantly diminishing its σ receptor targeting ability. Recently, we have used this strategy to modify estrogen receptor ligand, leading to the development of a highly potent, selective antibreast cancer agent.[28] Hence, this strategy of chemically modifying antagonists/agonists of other receptors that are overexpressed in various types of cancers could gain further importance in the development of potential anticancer therapeutics in future.

EXPERIMENTAL SECTION

Chemicals and General Procedures. Haloperidol was purchased from Sigma (St. Louis, MO, U.S.). 1-Bromopropane, 1-iodobutane, 1-bromooctane, 1-bromododecane, 1-bromohexadecane, and octan-1-amine were purchased from Alfa Aesar (Ward Hill, MA). HATU and glycine *tert*-butyl ester were purchased from Novabiochem (Germany). σ receptor siRNA (human) (against subtype 1, catalog no. SC-42250) was purchased from Santa Cruz Biotechnology (Santa Cruz, CA). This siRNA product is a mixture of three siRNAs with following sequences: (A) sense, GGAUAUCCAUGCUUAUGUAtt; antisense, UACAUAAGCAUGGAUAUCCtt; (B) sense, GUCCUCACCAUAUGCCUUAtt; antisense, UAAGGCAUAUGGUGAGGACtt; (C) sense, GGAACGAGAGUAAUUUGAAtt; antisense, UUCAAAUUACUCUCGUUCCtt. The universal negative control siRNA (catalog no. 1022076, sense sequence UUCUCCGAACGUGUCACGUTT, antisense sequence ACGUGACACGUUCGGAGAATT) was purchased from Qiagen (Valencia, CA). Antibodies were purchased from Santa Cruz Biotechnology. All other chemicals, reagents, and organic solvents were purchased either from Sigma (St. Louis, MO, U.S.) or from S. D. Fine Chemicals Ltd. (Mumbai, India). The reagents were >95% pure and were used without further purification. All the intermediates in the synthesis were characterized by ^{1}H NMR and/or mass spectrometry. The final molecules were characterized by ^{1}H NMR and ESI-HRMS, and the purity was ascertained by HPLC. ^{1}H NMR spectra were recorded on a Varian FT 200 MHz or Bruker FT 300 MHz spectrometer. Chemical shifts (δ) are reported in ppm relative to chloroform resonances (1H: 7.24 ppm for [D]chloroform). Data for ^{1}H NMR are reported as follows: chemical shift (δ in ppm), multiplicity (s = singlet, br s = broad singlet, d = doublet, t = triplet, q = quadruplet, m = multiplet), coupling constant (Hz), integration. ESI mass spectra were obtained using a QStar XL Hybrid QTOF mass spectrometer (Applied Biosystems). Purities of final products were clarified with a Varian ProStar HPLC instrument at 210 nm at a flow rate of 1 mL/min in a Varian Microsorb 100-10 BDS column (4.6 mm × 250 mm).

Chemistry. Synthesis of *tert*-Butyl 2-(Dibutylamino)acetate, 1a. Glycine *tert*-butyl ester (0.45 g, 3.43 mmol) was dissolved in 20 mL of dry ethyl acetate in a 50 mL round-bottomed flask fitted with a reflux condenser. Potassium carbonate (1.9 g, 13.77 mmol) and 1-iodobutane (2.56 g, 13.91 mmol) were added, and the resulting mixture was refluxed over an oil bath at 70−80 °C for 12 h. Then it was cooled and washed with water (2 × 20 mL) and brine (1 × 20 mL), dried over anhydrous Na_2SO_4, and evaporated. Column chromatographic purification of the residue using 60−120 mesh silica gel and 10% ethyl acetate−hexane (v/v) as eluent yielded compound **1a** as a colorless liquid (0.43 g, 51.4% yield, R_f = 0.6 in 30% ethyl acetate−hexane, v/v). ^{1}H NMR (300 MHz, $CDCl_3$): δ = 0.85−0.95 [t, 6H], 1.22−1.42 [m, 8H], 1.45 [s, 9H], 2.50−2.58 [t, 4H], 3.16 [s, 2H]. ESI-MS: m/z = 244 (calcd value for $C_{14}H_{29}O_2N$ = 243.2).

Synthesis of *tert*-Butyl 2-(Dioctylamino)acetate, 1b. *tert*-Butyl 2-(dioctylamino)acetate was synthesized following a similar procedure as for *tert*-butyl 2-(dibutylamino)acetate (64.2% yield, R_f = 0.65 in 30% ethyl acetate−hexane, v/v). ^{1}H NMR (300 MHz, $CDCl_3$): δ = 0.84−0.92 [t, 6H], 1.20−1.34 [m, 20H], 1.36−1.42 [m, 4H,], 1.45 [s, 9H], 2.46−2.56 [t, 4H], 3.16 [s, 2H]. ESI-MS: m/z = 357 (calcd value for $C_{22}H_{45}O_2N$ = 355.3).

Synthesis of *tert*-Butyl 2-(Didodecylamino)acetate, 1c. *tert*-Butyl-2-(didodecylamino)acetate was synthesized following a similar procedure as for *tert*-butyl 2-(dibutylamino)acetate (70.1% yield, R_f = 0.65 in 30% ethyl acetate−hexane, v/v). ^{1}H NMR (200 MHz, $CDCl_3$): δ = 0.82−0.95 [t, 6H], 1.13−1.40 [m, 36H], 1.44 [s, 9H], 1.45−1.65 [m, 4H], 2.45−2.58 [t, 4H], 3.16 [s, 2H]. ESI-MS: m/z = 468 (calcd value for $C_{30}H_{61}O_2N$ = 467.5).

Synthesis of *tert*-Butyl 2-(Dihexadecylamino)acetate, 1d. *tert*-Butyl 2-(dihexadecylamino)acetate was synthesized following a similar procedure as for *tert*-butyl-2-(dibutylamino)acetate (76.5% yield, R_f = 0.7 in 30% ethyl acetate−hexane, v/v). ^{1}H NMR (300 MHz, $CDCl_3$): δ = 0.84−0.92 [t, 6H], 1.20−1.36 [m, 52H], 1.45 [s, 9H], 1.55−1.65 [m, 4H], 2.48−2.56 [t, 4H], 3.16 [s, 2H]. ESI-MS: m/z = 581 (calcd value for $C_{38}H_{77}O_2N$ = 579.6).

Synthesis of *N*-(2-*tert*-Butoxy-2-oxoethyl)-*N*-butyl-*N*-methylbutan-1-aminium Iodide, 2a. Compound **1a** (0.43 g, 1.76 mmol) was dissolved in 5 mL of dry DCM in a 25 mL round-bottomed flask, and excess methyl iodide (3 mL) was added. The reaction mixture was stirred for 4 h at room temperature. Then it was concentrated and the residue upon column chromatographic purification using 60−120 mesh silica gel and 2% methanol−chloroform (v/v) as eluent, yielding compound **2a** as a yellowish gummy liquid (0.61 g, 89.6% yield, R_f = 0.4 in 10% methanol−chloroform, v/v). ^{1}H NMR (300 MHz, $CDCl_3$): δ = 1.00−1.08 [t, 6H], 1.40−1.51 [m, 4H], 1.53 [s, 9H], 1.75−1.90 [m, 4H], 3.60 [s, 3H], 3.73−3.90 [m, 4H], 4.56 [s, 2H]. ESI-MS: m/z = 258 (calcd value for $C_{15}H_{32}O_2N$ = 258.2).

Synthesis of *N*-(2-*tert*-Butoxy-2-oxoethyl)-*N*-methyl-*N*-octyloctan-1-aminium Iodide, 2b. Compound **2b** was synthesized following a similar procedure as for compound **2a** (86.7% yield, R_f = 0.45 in 10% methanol−chloroform, v/v). ^{1}H NMR (300 MHz, $CDCl_3$): δ = 0.84−0.92 [t, 6H], 1.20−1.42 [m, 20H], 1.53 [s, 9H], 1.70−1.88

[m, 4H], 3.61 [s, 3H], 3.64−3.88 [m, 4H], 4.60 [s, 2H]. ESI-MS: m/z = 371 (calcd value for $C_{23}H_{48}O_2N$ = 370.4).

Synthesis of *N*-(2-*tert*-Butoxy-2-oxoethyl)-*N*-dodecyl-*N*-methyldodecan-1-aminium Iodide, 2c. Compound **2c** was synthesized following a similar procedure as for compound **2a** (82.8% yield, R_f = 0.55 in 10% methanol−chloroform, v/v). ^{1}H NMR (200 MHz, $CDCl_3$): δ = 0.82−0.95 [t, 6H], 1.15−1.40 [m, 36H], 1.50 [s, 9H], 1.59−1.86 [m, 4H], 3.46−3.63 [m, 4H], 3.65 [s, 3H], 4.33 [s, 2H]. ESI-MS: m/z = 482 (calcd value for $C_{31}H_{64}O_2N$ = 482.5).

Synthesis of *N*-(2-*tert*-Butoxy-2-oxoethyl)-*N*-hexadecyl-*N*-methylhexadecan-1-aminium Iodide, 2d. Compound **2d** was synthesized following a similar procedure as for compound **2a** (80.5% yield, R_f = 0.6 in 10% methanol−chloroform, v/v). ^{1}H NMR (300 MHz, $CDCl_3$): δ = 0.84−0.92 [t, 6H], 1.19−1.44 [m, 52H], 1.52 [s, 9H], 1.68−1.88 [m, 4H], 3.61 [s, 3H], 3.64−3.88 [m, 4H], 4.61 [s, 2H]. ESI-MS: m/z = 595 (calcd value for $C_{39}H_{80}O_2N$ = 594.6).

Synthesis of *N*-(Carboxymethy)-*N*-butyl-*N*-methylbutan-1-aminium Trifluoroacetate, 3a. Compound **2a** (0.61 g, 1.58 mmol) was dissolved in 2 mL of dry DCM in a 25 mL round-bottomed flask and stirred over an ice bath for 15 min. Then 2 mL of trifluoroacetic acid was added dropwise to the solution. The reaction mixture was stirred over an ice bath for a further 15 min and then for 4 h at room temperature. DCM and excess trifluoroacetic acid were chased by nitrogen flushing. The residue was purified by flush column chromatography using 60−120 mesh silica gel and 8% methanol−chloroform (v/v) as eluent to obtain compound **3a** as a colorless gummy liquid (0.33 g, 66.4% yield, R_f = 0.3 in 10% methanol−chloroform, v/v). ESI-MS: m/z = 202 (calcd value for $C_{11}H_{24}O_2N$ = 202.2)

Synthesis of *N*-(Carboxymethyl)-*N*-methyl-*N*-octyloctan-1-aminium Trifluoroacetate, 3b. Compound **3b** was synthesized following a similar procedure as for compound **3a** (71.9% yield, R_f = 0.4 in 10% methanol−chloroform, v/v). ESI-MS: m/z = 315 (calcd value for $C_{19}H_{40}O_2N$ = 314.3).

Synthesis of *N*-(Carboxymethyl)-*N*-dodecyl-*N*-methyldodecan-1-aminium Trifluoroacetate, 3c. Compound **3c** was synthesized following a similar procedure as for compound **3a** (72.5% yield, R_f = 0.5 in 10% methanol−chloroform, v/v). ESI-MS: m/z = 426 (calcd value for $C_{27}H_{56}O_2N$ = 426.4).

Synthesis of *N*-(Carboxymethyl)-*N*-hexadecyl-*N*-methylhexadecan-1-aminium Trifluoroacetate, 3d. Compound **3d** was synthesized following a similar procedure as for compound **3a** (78.4% yield, R_f = 0.55 in 10% methanol−chloroform, v/v). ESI-MS: m/z = 539 (calcd value for $C_{35}H_{72}O_2N$ = 538.6).

Synthesis of *N*-Boc-*β*-alanine−Haloperidol Conjugate, 4. A mixture of *N*-Boc-*β*-alanine (0.91 g, 4.81 mmol), haloperidol (1.50 g, 3.99 mmol), and *N*,*N*-dimethylaminopyridine (DMAP) (0.24 g, 1.97 mmol) was dissolved in 10 mL of dry DCM in a 50 mL round-bottom flask and stirred in ice for half an hour. To the mixture, DCC (0.99 g, 4.8 mmol) dissolved in 5 mL of dry DCM was added, and the sample was stirred in an ice bath for 1 h. The reaction mixture was further stirred for 24 h at room temperature. Then the reaction mixture was filtered. The filtrate was washed with water (2 × 30 mL) and brine (1 × 30 mL), dried with anhydrous Na_2SO_4, and evaporated. Column chromatographic purification of the residue using 60−120 mesh silica gel and 1% methanol−chloroform (v/v) as eluent yielded compound **4** as a reddish-yellow gummy material (1.41 g, 64.6% yield, R_f = 0.6 in 5% methanol−chloroform, v/v). ^{1}H NMR (200 MHz, $CDCl_3$): δ = 1.43 [s, 9H], 1.75−2.05 [m, 4H], 2.15−2.55 [m, 8H], 2.65−2.80 [m, 2H], 2.85−3.00 [t, 2H], 3.2−3.35 [m, 2H], 4.70−4.90 [m, 1H], 7.05−7.35 [m, 6H], 7.90−8.05 [m, 2H]. ESI-MS: m/z = 547 (calcd value for $C_{29}H_{36}O_5N_2ClF$ = 546.2).

Synthesis of *β*-Alanine−Haloperidol Conjugate, 5. Compound **4** (1.41 g, 2.58 mmol) was dissolved in 18 mL of dry DCM in a 50 mL round-bottomed flask and stirred over an ice bath for 15 min. Then 2 mL of trifluoroacetic acid was added dropwise to the solution. The reaction mixture was further stirred over an ice bath for 4 h, and then the solution was neutralized using saturated $NaHCO_3$ solution. The mixture was extracted with DCM (2 × 15 mL), and the organic layer was dried with Na_2SO_4. Evaporation of the organic layer afforded compound **5** as a reddish-yellow gummy material (1.04 g, 90.4% yield, R_f = 0.1 in 5% methanol−chloroform, v/v, active in ninhydrin charring). Because compound **5** was obtained as 95% pure (revealed by TLC), it was directly used for the next step. ESI-MS: m/z = 447 (calcd value for $C_{24}H_{28}O_3N_2ClF$ = 446.2).

Synthesis of HP-C4. Compound **3a** (0.13 g, 0.41 mmol) was dissolved in 5 mL of dry DMF in a 25 mL round-bottomed flask and stirred over an ice bath for 15 min. To this, [dimethylamino(triazolo-[4,5-*b*]pyridine-3-yloxy)methylidene]dimethylazanium hexafluorophosphate (HATU) (0.17 g, 0.45 mmol) was added, and stirring was continued for another 30 min. Then compound **5** (0.27 g, 0.60 mmol) dissolved in 2 mL of dry DMF was added followed by dropwise addition of diisopropylethylamine (DIPEA) until the reaction mixture became slightly basic. The resulting mixture was stirred for 48 h. Then the reaction mixture was dissolved in 30 mL of DCM, washed with 1 N HCl (2 × 30 mL), water (1 × 30 mL), and brine (1 × 30 mL), dried with anhydrous Na_2SO_4, and evaporated. Column chromatographic purification (using >200 mesh silica gel and 2% methanol−chloroform, v/v, as eluent) of the residue followed by chloride ion exchange chromatography (using Amberlite IRA-400Cl resin and methanol as eluent) yielded HP-C4 as a colorless gummy solid (0.09 g, 32.7% yield, R_f = 0.45 in 10% methanol−chloroform, v/v). HPLC purity, >98%. ^{1}H NMR (300 MHz, $CDCl_3$): δ = 0.88−1.00 [t, 6H], 1.15−1.40 [m, 8H], 1.54−1.72 [m, 4H], 2.10−2.25 [m, 2H], 2.30−2.75 [m, 6H], 3.10 [s, 3H], 3.10−3.25 [m, 2H], 3.25−3.50 [m, 8H], 4.23 [s, 2H], 7.00−7.10 [t, 2H], 7.15−7.30 [m, 4H], 7.85−8.00 [m, 2H]. ESI-HRMS: m/z = 630.3471 (calcd value for $C_{35}H_{50}O_4N_3ClF$ = 630.3473).

Synthesis of HP-C8. HP-C8 was synthesized following similar procedure for the synthesis of HP-C4 (24.3% yield, R_f = 0.5 in 10% methanol−chloroform, v/v). ^{1}H NMR (300 MHz, $CDCl_3$): δ = 0.83−0.92 [t, 6H], 1.16−1.38 [m, 20H], 1.56−1.76 [m, 4H], 2.00−2.24 [m, 4H], 2.44−2.57 [m, 2H], 2.60−2.95 [m, 6H], 2.98−3.05 [m, 2H], 3.08 [s, 3H], 3.34−3.53 [m, 8H], 4.30 [s, 2H], 7.04−7.14 [t, 2H], 7.20−7.32 [m, 4H], 7.92−8.02 [m, 2H]. ESI-HRMS: m/z = 742.4746 (calcd value for $C_{43}H_{66}O_4N_3ClF$ = 742.4725). HPLC purity, >99%.

Synthesis of HP-C12. HP-C12 was synthesized following similar procedure for the synthesis of HP-C4 (16.2% yield, R_f = 0.6 in 10% methanol−chloroform, v/v). ^{1}H NMR (300 MHz, $CDCl_3$): δ = 0.82−0.95 [t, 6H], 1.17−1.38 [m, 30H], 1.55−1.74 [m, 4H], 1.95−2.26 [m, 4H], 2.45−2.59 [m, 2H], 2.61−2.96 [m, 6H], 2.98−3.05 [m, 2H], 3.07 [s, 3H], 3.34−3.51 [m, 8H], 4.25 [s, 2H], 7.04−7.14 [t, 2H], 7.21−7.30 [m, 4H], 7.91−8.01 [m, 2H]. ESI-HRMS: m/z = 854.6000 (calcd value for $C_{51}H_{82}O_4N_3ClF$ = 854.5977). HPLC purity, >98%

Synthesis of HP-C16. HP-C16 was synthesized following similar procedure for the synthesis of HP-C4 (13% yield, R_f = 0.65 in 10% methanol−chloroform, v/v). ^{1}H NMR (200 MHz, $CDCl_3$): δ = 0.78−0.93 [t, 6H], 1.12−1.41 [m, 52H], 1.53−1.77 [m, 4H], 1.96−2.27 [m, 4H], 2.39−2.54 [m, 2H], 2.61−2.85 [m, 6H], 2.90−3.05 [m, 2H], 3.06 [s, 3H], 3.30−3.55 [m, 8H], 4.34 [s, 2H], 7.04−7.16 [t, 2H], 7.23−7.33 [m, 4H], 7.91−8.03 [m, 2H]. ESI-MS: m/z = 966.7216 (calcd value for $C_{59}H_{98}O_4N_3ClF$ = 966.7229). HPLC purity, >99%.

Synthesis of Dioctylamine, 7. A mixture of octan-1-amine (2 g, 15.5 mmol), 1-bromooctane (2.98 g, 15.5 mmol), and anhydrous potassium carbonate (2.34 g, 18.01 mmol) in 4 mL of DMSO was kept under stirring for 12 h at 80 °C. The reaction mixture was taken in 50 mL of chloroform, washed with water (3 × 50 mL), dried over anhydrous Na_2SO_4, and evaporated. Column chromatographic purification of the residue using 60−120 mesh silica gel and 1% methanol−chloroform (v/v) as eluent afforded compound **7** as a white solid (1.3 g, 30.8% yield,

R_f = 0.55 in 10% methanol−chloroform, v/v). ^{1}H NMR (200 MHz, $CDCl_3$): δ = 0.9 [t, 6H], 1.05−1.45 [m, 20H], 1.6−1.85 [m, 4H], 2.8 [t, 4H].

Synthesis of *N*-Octyl-*N*-propyloctan-1-amine, 8. In a 50 mL round-bottomed flask a mixture of compound **7** (0.5 g, 2.07 mmol), 1-bromopropane (0.381 g, 3.1 mmol), and anhydrous potassium carbonate (0.55 g, 4.14 mmol) in 10 mL of ethyl acetate was kept under stirring for 24 h at 70 °C. Then the solvent was evaporated. Column chromatographic purification of the residue using 60−120 mesh silica gel and 10% ethyl acetate in hexane (v/v) as the eluent afforded compound **8** as a white solid (0.55 g, 77.8% yield, R_f = 0.6 in 30% ethyl acetate−hexane, v/v). ^{1}H NMR (200 MHz, $CDCl_3$): δ = 0.9 [t, 9H], 1.05−1.45 [m, 20H], 1.4−1.6 [m, 6H], 2.2−2.4 [m, 6H].

Synthesis of C8 Control, 9. Compound **8** (0.5 g, 1.46 mmol) was dissolved in 5 mL of dry DCM and treated with excess methyl iodide (3 mL) and stirred for 4 h at room temperature. Then the reaction mixture was concentrated. Column chromatographic purification of the residue (using 100−200 mesh silica gel and 1% methanol−chloroform (v/v) as eluent) followed by chloride ion exchange chromatography (using Amberlite IRA-400Cl resin and methanol as eluent) yielded the C8 control molecule (**9**) as a light yellow gummy solid (0.22 g, 40% yield, R_f = 0.3 in 10% methanol−chloroform, v/v). ^{1}H NMR (200 MHz, $CDCl_3$): δ = 0.9 [t, 6H], 1−1.1 [t, 3H], 1.2−1.5 [m, 20H], 1.65−1.9 [m, 6H], 3.5−3.6 [m, 6H], 3.4 [s, 3H]. ESI-HRMS: m/z = 298.3473 (calcd value for $C_{20}H_{44}N$ = 298.3473). HPLC purity >98%.

Biology. *Preparation of Samples and Sample Treatment.* The compounds were dissolved in cell culture grade DMSO to get a primary stock. The stock is progressively diluted with DMSO to get secondary stocks. Finally, the working concentrations of the derivatives were obtained by adding the secondary DMSO stocks in 10% fetal bovine serum containing cell culture medium. The amount of DMSO in working solutions never exceeded more than 1% with respect to the serum containing culture medium. For the viability studies an amount of 100 μL of cell culture solutions containing respective concentrations of compounds was added to each well of 96-well plates. For quantification of apoptosis studies an amount of 1.5 mL of culture medium containing respective concentration of compounds was added to each well of 6-well plates.

Cell Culture. MCF-7, MDA-MB-231, ZR-75-1, B16F10, COS-1, and HEK-293 cells were purchased from the National Center for Cell Sciences (Pune, India) and were mycoplasma free. Cells were cultured in RPMI-1640 medium (Sigma) supplemented with 10% fetal bovine serum (GIBCO), 50 μg/mL penicillin, 50 μg/mL streptomycin, and 100 μg/mL kanamycin at 37 °C in a humidified atmosphere of 5% CO_2 in air. Cultures of 85−90% confluency were used for all of the experiments. The cells were trypsinized, counted, and seeded in 96-well plates for viability studies, in 6-well plates for quantification of apoptosis studies, and in 100 × 20 mm^2 tissue culture Petri dish for Western blot studies. The cells were allowed to adhere overnight before they were used for experiments. HUVEC cells (Lonza Inc.) were cultured in company recommended medium, EGM (endothelial growth medium)-2 Bullet Kit (Lonza Inc.), and were maintained as described above. HUVEC cell-based experiments were done in second and third cellular passages only.

Cytotoxicity Studies. Cytotoxicities of the compounds were evaluated by the 3-(4,5-dimethylthiazol-2-yl)-2,5-diphenyltetrazolium bromide (MTT) reduction assay. Briefly, cells were seeded at a density of 5000 cells/well in a 96-well plate usually 18−24 h before experiment. Solutions containing respective concentrations of compounds were added to triplicate wells. In the screening studies derivatives of haloperidol were continuously treated to the cells for 48 h. In other studies, cytotoxic cationic haloperidol derivative HP-C8 along with haloperidol and C8 control was continuously treated for 48 h. Following the termination of experiment cells were washed and promptly assayed for viability using MTT. Results were expressed as percent viability = $\{[A_{540}(\text{treated cells}) - \text{background}]/[A_{540}(\text{untreated cells}) - \text{background}]\} \times 100$.

σ Receptor Down-Regulation by siRNA Delivery. siRNA based σ receptor down-regulation was performed following a similar procedure described earlier.[19] In brief, MCF-7 or COS-1 cells were seeded at a density of 2 × 10^5 cells per well in a 6-well plate usually between 18 and 24 h before transfection. Then 5 pmol of σ receptor siRNA (subtype 1) (Santa Cruz Biotechnology) or 5 pmol of negative control siRNA (Qiagen) (diluted to 50 μL with serum free RPMI) was complexed with 0.5 μL of Lipofectamine 2000 (Invitrogen) (diluted to 50 μL with serum free RPMI) for 15 min. An amount of 900 μL of serum free RPMI was added to the resulting complex. Cells were washed with phosphate-buffered saline (PBS) and then treated with respective complexes. After 4 h of incubation, cells were harvested, counted, and again seeded at a density of 10 000 cells per well in 96-well plates for cytotoxicity assay. After 16−18 h cells were kept untreated or treated with 10 μM HP-C8 for 4 h. After 4 h of treatment, the cells were washed and kept in the presence of fresh cell culture medium for 48 h. The cells were then assayed for viability using MTT as described earlier.

Flow Cytometric Analysis. The remaining cells after seeding from the above experiment were used to evaluate the extent of down-regulation of σ receptor by flow cytometry. They were replated, and after 24 h they were harvested, washed, fixed with 2% formaldehyde, and kept at 4 °C for 2 h. Then they were collected by centrifugation, washed, and treated with polyclonal antibody raised against full-length σ receptor of human origin in rabbit (Santa Cruz Biotechnology) at 1:100 dilution (in PBS containing 2% fetal bovine serum). After incubating at 4 °C for 2 h, cells were collected by centrifugation, washed, and treated with FITC conjugated goat-antirabbit secondary antibody (Santa Cruz Biotechnology) at 1:200 dilution (in PBS containing 2% fetal bovine serum) and incubated at 4 °C for 1 h in the dark. Finally cells were analyzed using a flow cytometer (FACS Canto II, Becton Dickinson, San Jose, CA, U.S.) and data were analyzed with FCS Express V3 software. A minimum of 10 000 events were gated per sample.

Quantification of Apoptosis Studies. The annexin V-FITC-labeled apoptosis detection kit (Sigma) was used to detect and quantify apoptosis by flow cytometry per manufacturer's instructions. In brief, cells (2 × 10^5 cells/well) were seeded in six-well plates and cultured overnight in 10% serum medium. After 16−18 h cells were kept untreated or treated with 5 μM haloperidol or 5 μM HP-C8 for 24 h. Then the cells were harvested and collected by centrifugation for 5 min at 1000*g*. Cells were then resuspended at a density of 1 × 10^6 cells/mL in 1× binding buffer and stained simultaneously with FITC-labeled annexin V (25 ng/mL) and propidium iodide (50 ng/mL). Cells were analyzed using a flow cytometer (FACS Canto II), and data were analyzed with FCS Express V3 software. A minimum of 10 000 events were gated per sample.

Preclinical Studies Using C57BL6/J Mice. Male C57BL6/J mice were obtained from CCMB (Hyderabad, India). The protocols for animal experimentations were approved through Institutional Animal Ethical Committee. Male C57BL6/J mice, 6−8 weeks old, were subcutaneously inoculated with 2 × 10^5 B16F10 cells in the lower right abdomen. Eleven days following cancer cell implantation, mice were grouped as per treatment. The groups were as follows: (i) group treated with haloperidol (four mice) and (ii) group treated with HP-C8 (four mice). For each treatment group an amount of 7.5 mg/kg respective compounds suspended in PBS containing 10% DMSO was injected. Five intraperitoneal injections with a gap of 2−3 days were administered. Tumors were measured three times a week. The tumor sizes were expressed in volume (mm^3) and calculated using the formula ($0.5ab^2$), where a is the longest dimension and b is the shortest dimension of the tumors. Experiment was terminated when the average tumor volume of the haloperidol treated group reached ∼4000 mm^3.

TUNEL Assay. After completion of the above experiment one mouse from each group was sacrificed for detection of apoptosis in tumor tissues.

The tumors were frozen in Jung tissue freeze medium (Leica Microsystem, Germany) followed by cryosectioning of 10 μm thin sections using Leica CM1850 cryostat (Germany). The sections were fixed and TUNEL assayed using DeadEnd fluorometric TUNEL assay kit (Promega, Madison, WI) per manufacturer's protocol. Images were acquired in Nikon TE2000E microscope at 10× magnification.

Western Blot. For this study, both B16F10 and HUVEC cells were treated with HP or HP-C8 (10 μM) or kept untreated for 24 h in charcoal stripped serum condition (RPMI for B16F10 and EBM solution with bullet kit (Lonza) except the recommended serum). Following treatment whole cell lysates from both the cells were prepared as follows: Cells were lysed with cold radioimmunoprecipitation assay buffer (RIPA, Boston BioProducts, MA, U.S.) (50 mM Tris-HCl, pH 7.4, 0.15 M NaCl, 1% Nonidet P-40, 0.5% sodium deoxycholate, and 0.1% SDS), which was premixed with 1× Halt phosphatase inhibitor cocktail, 1× protease inhibitor cocktail (Thermo Scientific, IL, U.S.), and 2 mM sodium vanadate. Respective cell lysates were run in SDS-PAGE gradient gel, and then the bands were transferred to PVDF membrane. Antibodies such as caspase 3, Bax, Akt1/2/3, and pAkt1/2/3 (Santa Cruz), Bcl-2 (Cell Signaling Technology, Beverly, MA), and anti-β-actin (Sigma Chemical Company, St. Louis, MO) followed by horseradish peroxidase conjugated secondary antibody (Santa Cruz Biotechnology) and the SuperSignal West Pico substrate (Pierce Biotechnology) were used for detection of protein bands.

Statistical Analysis. Data were expressed as the mean ± SD and statistically analyzed by the two-tailed, unpaired, Student's *t*-test using Microsoft Excel (Seattle, WA). For animal studies, scores were considered significant when $p < 0.05$. For in vitro studies, scores were considered significant when $p < 0.01$.

■ ASSOCIATED CONTENT

Supporting Information. Detailed spectral characterization data and HPLC purity data of all final molecules; Figure S1 depicting toxicity comparison of HP-C8 with mixture of HP and C8-molecule in B16F10 cell. This material is available free of charge via the Internet at http://pubs.acs.org.

■ AUTHOR INFORMATION

Corresponding Author

*Phone: 91-40-27191476. Fax: 91-40-27193370. E-mail: rkbanerjee@yahoo.com and banerjee@iict.res.in.

Present Addresses

[||]Department of Biochemistry and Molecular Biology, Mayo Clinic Foundation, Rochester, Minnesota 55902, U.S.

■ ACKNOWLEDGMENT

K.P. and S.K.P thank CSIR, Government of India, for their doctoral fellowship. R.B. thanks Department of Science and Technology, Government of India, for research support (Grant SR/S1/OC-64/2008).

■ ABBREVIATIONS USED

HP, haloperidol; PI, propidium iodide; PI3K, phosphatidylinositol 3-kinase; Akt, protein kinase B; HUVEC, human umbilical cord vascular endothelial cell; FITC, fluorescein isothiocyanate; TUNEL, terminal deoxynucleotide transferase dUTP nick end labeling; Bcl-2, B-cell lymphoma 2; BAX, Bcl-2-associated X protein

■ REFERENCES

(1) Wolfe, S. A., Jr.; Culp, S. G.; De Souza, E. B. Sigma-receptors in endocrine organs: identification, characterization, and autoradiographic localization in rat pituitary, adrenal, testis, and ovary. *Endocrinology* **1989**, *124*, 1160–1172.

(2) Hellewell, S. B.; Bruce, A.; Feinstein, G.; Orringer, J.; Williams, W.; Bowen, W. D. Rat liver and kidney contain high densities of sigma 1 and sigma 2 receptors: characterization by ligand binding and photoaffinity labeling. *Eur. J. Pharmacol.* **1994**, *268*, 9–18.

(3) Vilner, B. J.; John, C. S.; Bowen, W. D. Sigma-1 and sigma-2 receptors are expressed in a wide variety of human and rodent tumor cell lines. *Cancer Res.* **1995**, *55*, 408–13.

(4) John, C. S.; Bowen, W. D.; Saga, T.; Kinuya, S.; Vilner, B. J.; Baumgold, J.; Paik, C. H.; Reba, R. C.; Neumann, R. D.; Varma, V. M.; McAfee, J. G. A malignant melanoma imaging agent: synthesis, characterization, in vitro binding and biodistribution of iodine-125-(2-piperidinylaminoethyl)4-iodobenzamide. *J. Nucl. Med.* **1993**, *34*, 2169–2175.

(5) John, C. S.; Vilner, B. J.; Bowen, W. D. Synthesis and characterization of [^{125}I]-*N*-(*N*-benzylpiperidin-4-yl)-4-iodobenzamide, a new sigma receptor radiopharmaceutical: high affinity binding to MCF-7 breast tumor cells. *J. Med. Chem.* **1994**, *37*, 1737–1739.

(6) John, C. S.; Vilner, B. J.; Gulden, M. E.; Efange, S. M.; Langason, R. B.; Moody, T. W.; Bowen, W. D. Synthesis and pharmacological characterization of 4-[^{125}I]-*N*-(*N*-benzylpiperidine-4-yl)-4-iodobenzmide: a high affinity sigma receptor ligand for potential imaging of breast cancer. *Cancer Res.* **1995**, *55*, 3022–3027.

(7) John, C. S.; Gulden, M. E.; Vilner, B. J.; Bowen, W. D. Synthesis, in vitro validation and in vivo pharmacokinetics of [^{125}I]*N*-[2-(4-iodophenyl)ethyl]-*N*-methyl-2-(1-piperidinyl)ethylamine: a high-affinity ligand for imaging sigma receptor positive tumors. *Nucl. Med. Biol.* **1996**, *23*, 761–766.

(8) John, C. S.; Vilner, B. J.; Geyer, B. C.; Moody, T.; Bowen, W. D. Targeting sigma receptor-binding benzamides as in vivo diagnostic and therapeutic agents for human prostate tumors. *Cancer Res.* **1999**, *59*, 4578–4583.

(9) John, C. S.; Bowen, W. D.; Fisher, S. J.; Lim, B. B.; Geyer, B. C.; Vilner, B. J.; Wahl, R. L. Synthesis, in vitro pharmacologic characterization, and preclinical evaluation of *N*-[2-(1′-piperidinyl)ethyl]-3-[^{125}I]iodo-4-methoxybenzamide (P[125I]MBA) for imaging breast cancer. *Nucl. Med. Biol.* **1999**, *26* (4), 377–382.

(10) Wheeler, K. T.; Wang, L. M.; Wallen, C. A.; Childers, S. R.; Cline, J. M.; Keng, P. C.; Mach, R. H. Sigma-2 receptors as a biomarker of proliferation in solid tumours. *Br. J. Cancer* **2000**, *82*, 1223–1232.

(11) Zamora, P. O.; Moody, T. W.; John, C. S. Increased binding to sigma sites of *N*-[1′(2-piperidinyl)ethyl)-4-[I-125]-iodobenzamide (I-125-PAB) with onset of tumor cell proliferation. *Life Sci.* **1998**, *63*, 1611–1618.

(12) Crawford, K. W.; Bowen, W. D. Sigma-2 receptor agonists activate a novel apoptotic pathway and potentiate antineoplastic drugs in breast tumor cell lines. *Cancer Res.* **2002**, *62*, 313–322.

(13) Brent, P. J.; Pang, G. T. Sigma binding site ligands inhibit cell proliferation in mammary and colon carcinoma cell lines and melanoma cells in culture. *Eur. J. Pharmacol.* **1995**, *278*, 151–160.

(14) Wei, Z.; Mousseau, D. D.; Dai, Y.; Cao, X.; Li, X. M. Haloperidol induces apoptosis via the sigma2 receptor system and Bcl-XS. *Pharmacogenomics J.* **2006**, *6*, 279–288.

(15) Nordenberg, J.; Perlmutter, I.; Lavie, G.; Beery, E.; Uziel, O.; Morgenstern, C.; Fenig, E.; Weizman, A. Anti-proliferative activity of haloperidol in B16 mouse and human SK-MEL-28 melanoma cell lines. *Int. J. Oncol.* **2005**, *27*, 1097–1103.

(16) Dai, Y.; Wei, Z.; Sephton, C. F.; Zhang, D.; Anderson, D. H.; Mousseau, D. D. Haloperidol induces the nuclear translocation of phosphatidylinositol 3′-kinase to disrupt Akt phosphorylation in PC12 cells. *J. Psychiatry Neurosci.* **2007**, *32*, 323–330.

(17) Mukherjee, A.; Prasad, T. K.; Rao, N. M.; Banerjee, R. Haloperidol-associated stealth liposomes: a potent carrier for delivering genes to human breast cancer cells. *J. Biol. Chem.* **2005**, *280*, 15619–15627.

(18) Karmali, P. P.; Chaudhuri, A. Cationic liposomes as non-viral carriers of gene medicines: resolved issues, open questions, and future promises. *Med. Res. Rev.* **2007**, *27*, 696–722.

(19) Mukherjee, A.; Narayan, K. P.; Pal, K.; Kumar, J. M.; Rangaraj, N.; Kalivendi, S. V.; Banerjee, R. Selective cancer targeting via aberrant behavior of cancer cell-associated glucocorticoid receptor. *Mol. Ther.* **2009**, *17*, 623–631.

(20) Pham, T. Q.; Berghofer, P.; Liu, X.; Greguric, I.; Dikic, B.; Ballantyne, P.; Mattner, F.; Nguyen, V.; Loc'h, V.; Katsifis, A. Preparation and biologic evaluation of a novel radioiodinated benzylpiperazine, ^{123}I-MEL037, for malignant melanoma. *J. Nucl. Med.* **2007**, *48*, 1348–1356.

(21) Kim, N. R.; Park, S. W.; Lee, J. G.; Kim, Y. H. Protective effects of olanzapine and haloperidol on serum withdrawal-induced apoptosis in SH-SY5Y cells. *Prog. Neuropsychopharmacol. Biol. Psychiatry* **2008**, *32*, 633–642.

(22) Wei, Z.; Qi, J.; Dai, Y.; Bowen, W. D.; Mousseau, D. D. Haloperidol disrupts Akt signalling to reveal a phosphorylation-dependent regulation of pro-apoptotic Bcl-XS function. *Cell. Signallling* **2009**, *21*, 161–168.

(23) Brent, P. J.; Pang, G.; Little, G.; Dosen, P. J.; Van Helden, D. F. The sigma receptor ligand, reduced haloperidol, induces apoptosis and increases intracellular-free calcium levels [Ca^{2+}] in colon and mammary adenocarcinoma cells. *Biochem. Biophys. Res. Commun.* **1996**, *219*, 219–226.

(24) Kim, R.; Emi, M.; Tanabe, K. Role of mitochondria as the gardens of cell death. *Cancer Chemother. Pharmacol.* **2006**, *57*, 545–553.

(25) Gross, A.; McDonnell, J. M.; Korsmeyer, S. J. BCL-2 family members and the mitochondria in apoptosis. *Genes Dev.* **1999**, *13*, 1899–1911.

(26) Testa, J. R.; Bellacosa, A. Akt plays a central role in tumorigenesis. *Proc. Natl. Acad. Sci. U.S.A.* **2001**, *98*, 10983–10985.

(27) Riesterer, O.; Zingg, D.; Hummerjohann, J.; Bodis, S.; Pruschy, M. Degradation of PKB/Akt protein by inhibition of the VEGF receptor/mTOR pathway in endothelial cells. *Oncogene* **2004**, *23*, 4624–4635.

(28) Sinha, S.; Roy, S.; Reddy, B. S.; Pal, K.; Sudhakar, G.; Iyer, S.; Dutta, S.; Wang, E.; Vohra, P. K.; Roy, K. R.; Reddanna, P.; Mukhopadhyay, D.; Banerjee, R. A lipid modified estrogen derivative that treats breast cancer independent of estrogen receptor expression through simultaneous induction of autophagy and apoptosis. *Mol. Cancer Res.* [Online early access]. DOI: 10.1158/1541-7786.MCR-10-0526. Published Online: February 2, **2011**.